Fractional viscoelastic characterization of laminated glass beams under time-varying loading

Fractional viscoelastic characterization of laminated glass beams under time-varying loading

Mario Di Paola

Department of Engineering, University of Palermo
Viale delle Scienze, I 90128 Palermo, Italy

Laura Galuppi

Department of Engineering and Architecture, University of Parma
Parco Area delle Scienze 181/A, I 43100 Parma, Italy

Gianni Royer Carfagni*

Department of Engineering and Architecture, University of Parma
Parco Area delle Scienze 181/A, I 43100 Parma, Italy
and
Construction Technologies Institute - National Research Council of Italy (ITC-CNR)
Viale Lombardia 49, I 20098 San Giuliano Milanese, Italy

Abstract

Laminated glass is a composite made of elastic glass layers sandwiching thin viscoelastic polymeric interlayers. There are several types of polymers, traditionally modelled as linear viscoelastic materials using a Prony's series of units in the Maxwell-Wiechert arrangement. We show that one single element with fractional viscoelastic properties (two constitutive parameters that depend on environmental temperature), is sufficient to provide an accurate description of the polymer response under arbitrary time-varying actions. This is a great advantage over the classical viscoelastic

*Corresponding author.
Email addresses: mario.dipaola@unipa.it (Mario Di Paola), laura.galuppi@unipr.it (Laura Galuppi), gianni.royer@unipr.it (Gianni Royer Carfagni)

December 8, 2020

characterization, which requires at least 10-15 terms in the Prony's series, each one characterized by a relaxation time, so that the series covers the time-scale of the applied actions. Fractional viscoelasticity is incorporated in the analytical model of a three-layer laminated beam, susceptible of a zig-zag warping of the cross section, which is analyzed under time-dependent loading. The great potential of this approach is demonstrated in representative case studies.
Keywords: Viscoelasticity; fractional calculus; laminated glass; sandwich beams; polymeric interlayers.

---

1. Introduction

Laminated Glass (LG) is a structure composed by two (or more) glass plies sandwiching one (or more) thermoplastic polymeric interlayers [1], permanently bonded with a process at high temperature and pressure in autoclave (lamination) thanks to the chemical union of the hydroxil groups of the polymer with the silanol group on the glass surface. This is a safety glass, because even in the event of glass breakage, the fragments remain attached to the polymer ensuring a certain degree of cohesion [2], which prevents detachment from fixings and risks of injuries. Indeed, even in the pre-glass-breakage phase the thin polymeric interlayer, although too soft to provide axial and flexural stiffness per se, acts as a glue film, restraining the shear-sliding of the glass plies [3]. This increases the bending capacity of LG, which varies between the lower limit of free-sliding glass plies (*layered limit*), for which the flexural inertia is the sum of the inertiae of the glass layers, and the opposite upper-bound limit of perfectly coupled glass plies (*monolithic limit*), whose inertia corresponds to the total cross section of the glass spaced by the thicknesses of the interlayers.

The evaluation of the degree of bonding provided by the polymer in the laminate before glass breakage is one of the most classic topics [4] in the engineering science

of structural glass. Homogenized models based on the first-order [5] or higher-order [6] shear-deformation theory have been proposed, but in general the most effective approach shall consider the layerwise effect: the glass plies are structural beams [7] or plates [8], shear-coupled through the soft and thin polymeric interlayers. The compliance of the polymer provides a zig-zag warping in the thickness of the laminate, which is qualitative different from the smooth shapes predicted by shear deformation theory when the interlayer is soft beyond a certain limit [9].

There are many types of polymeric films [10]. The most used for structural applications are the polyvinyl butyral (PVB), the ionoplast SentryGlas (SG) and the ethylene-vinyl acetate (EVA), with many variations depending on the amount of added softeners and metal salts, and type of secondary processing. Since they are all highly viscoelastic, the response of LG is greatly affected by the load duration and operating temperature [11]. The rheological properties can be considered at different levels of complexity. A widely-used engineering approach is the *quasi-elastic* method [12], which treats the polymer as a linear elastic material with temperature- and time-dependent stiffness, coinciding with the secant value in *relaxation* tests at operating temperature, measured at a time corresponding to the design duration of the applied actions. This approximation is accepted in the widely used engineering methods for structural design that define the *effective thickness* of LG [7], i.e., the thickness of a monolith with equivalent bending properties in terms of stress and deflection. More refined rheological analyses are based on linear viscoelasticity theory, which typically assumes a volumetric-deviatoric elastic-viscoelastic split, such that only the deviatoric part affects the shear coupling of the glass plies through the interlayer [13]. The agreement with the quasi-elastic models, independently [14] of the structural theories used for the glass layers (Kirchhoff-Love, von Kármán, Reissner-Mindlin), is satisfactory under monotonic loading, but not when the load changes sign [15]. In fact, the quasi-elastic approach cannot consider the memory effect of viscoelasticity.

Since the early pioneering works [16, 17], the viscoelastic constitutive laws for the interlayers have been *dogmatically* interpreted through Prony's series of units in the Maxwell-Wiechert arrangement [18]. The parameters of the series can be calibrated via creep or relaxation tests [11], or by using a Dynamic Mechanical Analysis (DMA) of the response to cyclic oscillations [19]. The Williams Landel Ferry (WLF) equation [20], which establishes a correlation between the time scale of the rheological phenomenon and the operating temperature, is traditionally used to shift the time-dependent shear-modulus curve to a different temperature and/or to extrapolate the observations from short to longer times [11]. However, for a satisfactory interpolation of the experimental points, at least $10 - 15$ terms of the Prony's series are required. Each term in the series is characterized by two parameters, representing the relaxation shear modulus and the relaxation time. The number of terms shall be such that the relaxation times cover the duration of the actions throughout the entire life time of LG, ranging from a few seconds, as in the case of wind actions, to tens of years, for dead weight. Such a large number of coefficients are usually calibrated by using regression algorithms based on simplifying assumptions [21]. Furthermore, when laminated glass is subjected to actions of very short duration (hundredths of seconds), such as in the case of impacts or under a blast wave [22], terms in the series with relaxation times of the order of 10^{-5} s are necessary [23]. Since it is difficult to measure the relaxation curve for such short times, their evalutation would require DMA at extremely high frequencies, which can cause the specimens to heat up and, therefore, a variation in the material mechanical properties. As a matter of fact, analyzing the technical literature to the best of our knowledge, it is not clear how they are obtained, so much so that we are led to believe that they are generally proposed on the basis of experience or empirical rules.

In a famous article [24], Nutting was perhaps the first to observe that the experimental creep curves of many materials, like concrete, rubber and polymers, could

very well be fitted by a power-law; on the other hand, each term in the Prony's series provides an exponential dependence, characterized by a jump-like response at the corresponding relaxation time. Put simply, the difficulty in approximating the relaxation/creep curves of real polymers with a Prony's series stems from the fact that one is trying to interpolate power-laws with a series of exponential functions. This is obviously not natural and, therefore, it is not surprising that many terms are required to obtain a reasonable interpolation. From a graphical point of view, in a bi-logarithmic stress-time plane, a power-law relaxation-curve is a straight line, while the interpolating curve for Prony's series is typically wavy. Indeed, some authors [25] have proposed a power-law pre-smoothing, i.e., a preliminary power-law-series representation of experimental data, to be subsequently fitted with a Prony's series model to increase accuracy, but the aforementioned difficulties persist.

There are theories of viscoelasticity [26], for which the relaxation/creep functions naturally turn out to be power-laws rather than exponentials, or the superposition of exponentials. Their peculiarity is that the corresponding viscoelastic constitutive laws are formulated in terms of integral-differential equations involving fractional, rather than ordinary, derivatives. If the creep/relaxation function is a power law of order α, with $0 < \alpha < 1$, the Boltzmann superposition principle provides a fractional differential characterization of the same order α. In this context, a wealth of theoretical [27–38] and experimental [24, 39, 40] work has been done. Although most engineers are probably unfamiliar with fractional calculus, solving differential equations governed by fractional derivatives, as it will be shown in the sequel, does not produce any relevant computational complication, provided that the appropriate mathematical tools are used. A comprehensive review of the applications of fractional calculus in the broad field of mechanics can be found in [41] and, for specific applications to linear viscoelasticity, in [42]. Analytical solutions and step-by-step integration techniques are also discussed in [43–45].

Our aim here is to present, in the simplest possible way, a laminated glass beam model in which the interlayer is governed by a fractional viscoelastic constitutive law. After recalling in Section 2 the basic equations of fractional calculus applied to viscoelasticity, Section 3 is dedicated to the structural model of the laminated-glass beam. The numerical approach used to approximate the time-history for deflection under varying loads is outlined in Section 4. The application examples, illustrated in Section 5, begin with the calibration of material parameters, obtained from relaxation tests of [11]. Remarkably, only two material parameters are sufficient to interpret the viscoelastic properties and, although the calibration is made from experimental observations of one day, the same model can be used to describe the effects of actions of very short (impulsive) duration, as well as for long term loads, at least as long as the polymer is sufficiently far from the glass transition temperature, and outside the branch of the relaxation/creep curve that corresponds to it according to the Williams Landel Ferry model [20]. Paradigmatic case studies are then illustrated. The main advantages of the fractional approach over other types of viscoelastic models based on Prony's series expansions, together with the proposals for future developments, are summarized in the Conclusion Section.

2. Preliminaries in fractional characterization of viscoelastic polymers

Some preliminary remarks about fractional viscoelasticity are reported for the sake of completeness. It has been observed [24] that real materials (rubber, polymers, steel...), under an assigned stress history $\tau(t) = \tau_0 \mathcal{U}(t)$, where $\mathcal{U}(t)$ is the unit step function and, conventionally, $\tau_0 = 1\,\mathrm{Pa}$, exhibit a strain response $G(t)$ that, with a notation propaedeutic for the following developments, can be expressed as

$$G(t) = \frac{t^\alpha}{C_\alpha\ \Gamma(1+\alpha)}\,,\ \ (0 \le \alpha \le 1)\,, \tag{2.1}$$

where $\Gamma(\cdot)$ is the Euler's Gamma Function and C_α is a dimensional coefficient (here, $[C_\alpha] = \text{Pa s}^\alpha$). Both α and C_α can be obtained from best fitting with experimental data. The function $G(t)$ is referred to as the *creep function*. Once $G(t)$ is known, the Boltzmann superposition principle allows us to define the strain history $\gamma(t)$ associated with an assigned stress history $\tau(t)$, in the form

$$\gamma(t) = \frac{1}{C_\alpha \Gamma(1+\alpha)} \int_0^t (t-\bar{t})^\alpha \, \dot{\tau}(\bar{t}) \, d\bar{t} \,. \tag{2.2}$$

This expression is valid when the system is quiescent at $t = 0$, i.e., $\gamma(0) = 0$ and $\tau(0) = 0$. In the case that $\tau(0) \neq 0$, an extra term $G(t)\,\tau(0)$ has to be added on the r.h.s. of (2.2).

Integration by parts of (2.2) provides the constitutive law for the viscoelastic material that reads

$$\gamma(t) = \frac{1}{C_\alpha} \, {}_0\mathcal{I}_t^\alpha \left[\tau(\cdot)\right](t) \,, \tag{2.3}$$

where ${}_0\mathcal{I}_t^\alpha$ is the *Riemann-Liouville* (R-L) fractional integral, operating on any generic function $f(\cdot)$ according to

$${}_0\mathcal{I}_t^\alpha \left[f(\cdot)\right](t) = \frac{1}{\Gamma(\alpha)} \int_0^t (t-\bar{t})^{\alpha-1} \, f(\bar{t}) \, d\bar{t} \,. \tag{2.4}$$

If one supposes that the strain history is assigned in the form $\gamma(t) = \mathcal{U}(t)$, since $\gamma(t)$ remains constant for $t > 0$, the corresponding stress history will decay in time according to the *relaxation function*, referred to as $R(t)$ in the sequel. Using again the Boltzmann superposition principle, the stress history corresponding to an assigned strain history will be given by

$$\tau(t) = \int_0^t R(t-\bar{t})\dot{\gamma}(\bar{t})\, d\bar{t}\,. \tag{2.5}$$

The relaxation function $R(t)$ is strictly related to the creep function $G(t)$ by the fundamental law of viscoelasticity

$$\widehat{G}(s)\,\widehat{R}(s) = s^{-2}\,, \tag{2.6}$$

where $\widehat{G}(s)$ and $\widehat{R}(s)$ are the Laplace transform of $G(t)$ and $R(t)$, respectively, and s is the complex variable of the Laplace transform. With mathematical manipulations, one obtains that if $G(t)$ is of the form (2.1), the corresponding $R(t)$ is given by

$$R(t) = \frac{C_\alpha}{\Gamma(1-\alpha)} t^{-\alpha}\,. \tag{2.7}$$

Hence, inserting this expression in (2.5), one obtains

$$\tau(t) = C_\alpha\; {}_0^C\mathcal{D}_t^\alpha[\gamma(\cdot)](t)\,, \tag{2.8}$$

where ${}_0^C\mathcal{D}_t^\alpha$ is the Caputo's fractional derivative of order α, which is an operator transforming any function $f(\cdot)$ in

$${}_0^C\mathcal{D}_t^\alpha\left[f(\cdot)\right](t) = \frac{1}{\Gamma(1-\alpha)} \int_0^t (t-\bar{t})^{-\alpha}\, \dot{f}(\bar{t})\, d\bar{t}\,, \tag{2.9}$$

for $0 < \alpha < 1$. Also in this case, the expression is valid provided that $\gamma(0) = 0$, otherwise the extra term $\gamma(0)R(t)$ should be added on the r.h.s. of (2.8).

Equations (2.3) and (2.8) represent the constitutive laws of fractional viscoelasticity. A few remarks are useful.

i) As $\alpha = 0$, the linear elastic constitutive law is recovered; for $\alpha = 1$, the Newton-Petrof law for a purely viscous material is obtained. It follows that the intermediate value $0 < \alpha < 1$ provides and intermediate condition between the two aforementioned extreme (ideal) cases.

ii) For a quiescent system at $t = 0$, the R-L and the Caputo operators are the inverse one of the other.

iii) The operators (2.3) and (2.8) are linear and, hence, the main properties of the classical derivatives and integral of integer order (linearity, semigroup properties) are still valid, even if integration by parts and Leibniz rule in general do not hold true [46, 47].

iv) In the Laplace domain, they exactly behave as the classical derivatives and integrals; for example

$$\mathcal{L}\left\{\frac{d^n f}{dt^n}, s\right\} = (s)^n \hat{f}(s)\,, \quad \mathcal{L}\left\{{}_0^C\mathcal{D}_t^\alpha[f], s\right\} = (s)^\alpha \widehat{f}(s)\,, \tag{2.10}$$

provided that the values of $f(t)$ and its derivatives up to $n-1$ are null at $t = 0$.

With this in mind, it is now possible to consider the problem of the laminated glass beams, forming a composite structure where two linear elastic glass plies sandwich a viscoelastic interlayer.

3. The model of laminated glass beams under time-dependent loading

The considered model problem is that of a simply supported laminated glass beam of length L, composed by two external glass plies bonded by a polymeric interlayer, as schematically represented in Figure 1. In order to simplify the calculations, but without loosing generality, suppose that the two glass plies have the same thickness h

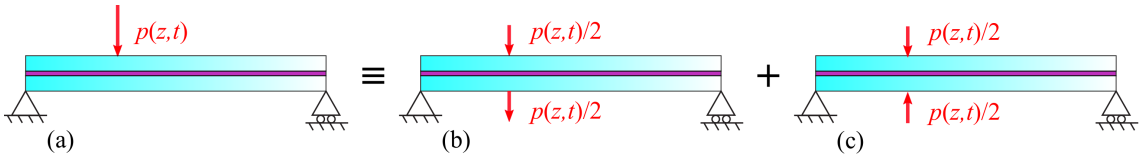

Figure 1: a) model problem of a simply supported laminated beam composed of two linear-elastic external layers bonded by a viscoelastic interlayer. Decomposition of the transversal applied load $p(z,t)$ in b) *antisymmetric* and c) *symmetric* components with respect to the horizontal middle plane.

and width b, while the thickness of the interlayer is set equal to rh, with $r \ll 1$. The glass plies are modelled as linear elastic Euler Bernoulli beams, for which E, $A = bh$, $I = bh^3/12$ represent the elastic modulus, the area and the moment of the inertia of the transversal cross section, respectively. The material forming the interlayer is viscoelastic, characterized through the creep function $G(t)$.

Introduce a reference frame (x, y, z) such that the z axis coincides with the centroidal line of the upper glass beam, the y axis is vertical and directed downwards, and the x is consequently oriented to render the reference system right-handed. As indicated in Figure 1, any generic vertical load $p(z,t)$ applied at one of the two glass plies can be considered, with respect to the horizonal middle plane of the laminate, as the sum of the *antisymmetric* part, consisting of $p(z,t)/2$ with concurring directions acting on each one of the plies and producing the bending of the beam, and the *symmetric* part, where the load $p(z,t)/2$ have opposite direction. The symmetric part is inessential for the bending of the beam if one assumes that the variation of the interlayer thickness consequent to its transversal axial deformation is negligible. Hence, only the antisymmetric case needs to be analyzed.

Consider, as shown in Figure 2, the free body diagram of the upper portion of the laminate isolated by the two cross sections at z and $z+dz$ and the horizontal symmetry plane, so that $-b/2 \leq x \leq b/2$ and $-h/2 \leq y \leq (1+r)h/2$. Let $p(z,t)/2$, $N(z,t)$,

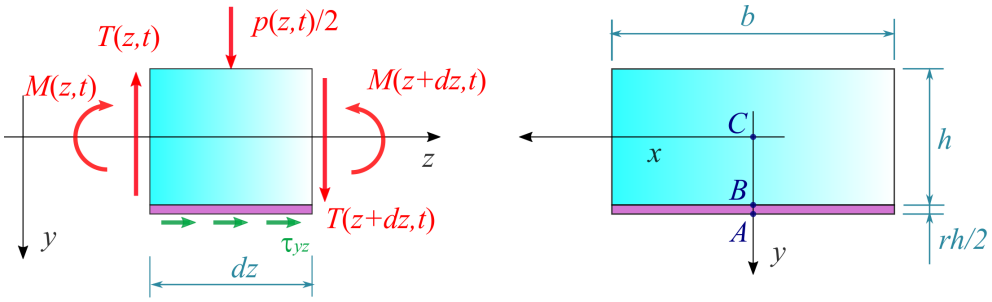

Figure 2: Free body diagram of the upper portion of the laminate identified by two neighboring cross sections and the horizontal symmetry plane. Longitudinal and transversal view.

$T(z,t)$ and $M(z,t)$ represent the transversal load per unit length, normal force, the shear force and the bending moment acting in the upper beam at the section z and the time t, respectively. Moreover, denote with $\tau_{yz}(z,t)$ the longitudinal shear stress component in the polymer at $y = (1+r)h/2$, supposed to be independent of the variable x.

The components on the reference frame (x,y,z) of the displacement field are denoted with $u(x,y,z,t)$, $v(x,y,z,t)$, $w(x,y,z,t)$, respectively. Points of interests are $A \equiv (0,(1+r)h/2,z)$, $B \equiv (0,h/2,z)$ and the centroid $C \equiv (0,0,z)$. Observe that

$$u\big(0,(1+r)h/2,z,t\big) = u_A(z,t) = 0\,, \tag{3.1a}$$

$$v\big(0,(1+r)h/2,z,t\big) = v\,(0,0,z,t) = v_C(z,t) = 0\,, \tag{3.1b}$$

$$w\big(0,(1+r)h/2,z,t\big) = w_A(z,t) = 0\,. \tag{3.1c}$$

The second condition is consistent with Euler-Bernoulli beam theory, while the others are due to symmetry with respect to the vertical and horizontal middle planes. It is immediate, from this Figure, to recognize that the shear stresses $\tau_{yz}(z,t)$ produces an action equipollent to a distributed axial force per unit length of the form

$n(z,t) = b\tau_{yz}(z,t)$ and to distributed couples per unit length equal to $m(z,x) = \frac{1}{2}(1+r)hb\tau_{yz}(z,t)$. Hence, the equilibrium equations become

$$\frac{\partial N(z,t)}{\partial z} = -n(z,t) = -b\tau_{yz}(z,t)\,, \tag{3.2a}$$

$$\frac{\partial T(z,t)}{\partial z} = \frac{1}{2}p(z,t)\,, \tag{3.2b}$$

$$\frac{\partial M(z,t)}{\partial z} = T(z,t) - m(z,t) = T(z,t) - \frac{(1+r)hb}{2}\tau_{yz}\,. \tag{3.2c}$$

The constitutive law for the interlayer is stated in terms of fractional calculus according to the definitions recalled in Section 2, and takes the form

$$\tau_{yz}(z,t) = C_\alpha\ {}_0^C\mathcal{D}_t^\alpha[\gamma_{yz}(z,\cdot)](t)\,, \tag{3.3}$$

where $\gamma_{yz}(z,t)$ is the shear strain in the polymer, supposed to be independent of the variables x and y from the hypothesis that $r \ll 1$.

The governing equations can be stated in terms of the vertical displacement of the centroidal line of the upper beam, for brevity indicated in the sequel as $v(z,t)$. If $\varphi(z,t)$ represents the rotation angle of the upper beam, considered positive if counterclockwise, by combining the classical constitutive equations for beam theory with the equilibrium conditions, one obtains

$$\frac{\partial v(z,t)}{\partial z} = -\varphi(z,t)\,, \tag{3.4a}$$

$$\frac{\partial^2 v(z,t)}{\partial z^2} = -\frac{M(z,t)}{EI}\,, \tag{3.4b}$$

$$\frac{\partial^3 v(z,t)}{\partial z^3} = -\frac{1}{EI}\left(T(z,t) - \frac{(1+r)hb}{2}\tau_{yz}(z,t)\right)\,, \tag{3.4c}$$

$$\frac{\partial^4 v(z,t)}{\partial z^4} = -\frac{1}{EI}\left(-\frac{p(z,t)}{2} - \frac{(1+r)hb}{2}\frac{\partial \tau_{yz}(z,t)}{\partial z}\right). \tag{3.4d}$$

In the simplest limit case in which the axial strain of the beam is supposed to be negligible, the interlayer strain $\gamma_{yz}(z,t)$ can be directly obtained as a function of $\varphi(z,t)$ by a simple geometric argument. Recalling (3.1c), from Figure 3 and (3.4a) one obtains

$$\gamma_{yz}(z,t) = -\frac{2}{rh}w_B(z,t) - \varphi(z,t) = -\frac{1+r}{r}\varphi(z,t) = \frac{1+r}{r}\frac{\partial v(z,t)}{\partial z}. \tag{3.5}$$

Hence, using (3.3) and (3.5), one finds from (3.4d) that the problem is solved by the fractional differential equation

$$\frac{\partial^4 v(z,t)}{\partial z^4} - C_\alpha \frac{(1+r)^2 hb}{2rEI}\,{}_0^C\mathcal{D}_t^\alpha\left[\frac{\partial^2 v}{\partial z^2}(z,\cdot)\right](t) = \frac{p(z,t)}{2EI}, \tag{3.6}$$

which contains only the transversal displacement $v(z,t)$. This is the simplest approach, which provides a fair approximation when r is sufficiently large and/or C_α is small, so that the shear coupling of the glass plies through the interlayer is moderate. In any case, this formulation represents an upper bound for the evaluation of the dissipated energy through the viscoelastic interlayer, since the shear strain γ_{yz} is here certainly underestimated.

A more realistic condition is that in which the tangential stress $\tau_{yz}(z,t)$ in the interlayer induces the axial force $N(z,t)$ in the upper glass beam and, by symmetry, an opposite force $-N(z,t)$ in the lower beam. The Euler-Bernoulli equations (3.4) remain unchanged, but (3.5) does not hold any more. In order to obtain the correct relationship, observe that the correct displacement at point B is given, as schematically illustrated in Figure 4, by

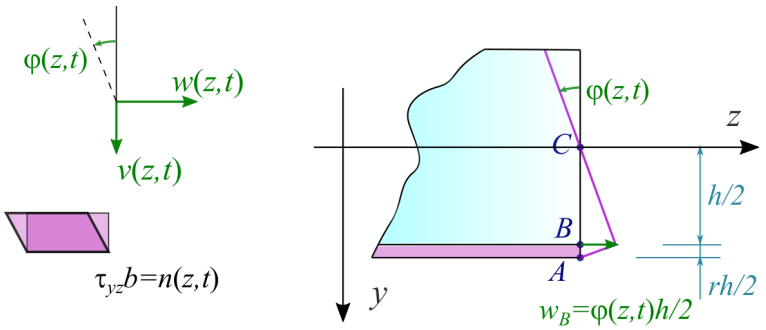

Figure 3: Geometric construction to calculate the interlayer shear strain $\gamma_{yz}(z,t)$ when the axial strain in the glass is neglected.

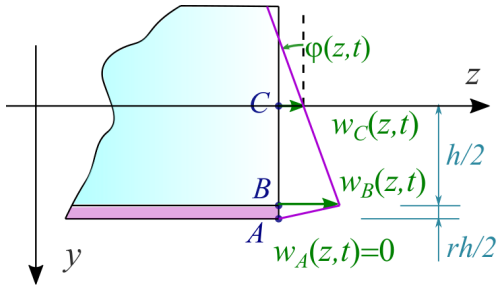

Figure 4: Displacement field at representative points of the interlayer when the axial deformation of the glass beam is considered.

$$w_B(z,t) = w_C(z,t) + \frac{h}{2}\varphi(z,t)\,. \tag{3.7}$$

Since, from the constitutive equations

$$\frac{\partial w_C(z,t)}{\partial z} = \frac{N(z,t)}{EA}\,, \quad \frac{\partial^2 w_C(z,t)}{\partial z^2} = -\frac{n(z,t)}{EA} = -\frac{b\tau_{yz}(z,t)}{EA}\,. \tag{3.8}$$

differentiating (3.7) with respect to z, one can write

$$\frac{\partial w_B(z,t)}{\partial z} = \frac{N(z,t)}{EA} + \frac{hM(z,t)}{2EI}\,, \tag{3.9}$$

Hence, with a similar argument that had led to (3.5), it follows that the shear strain in the interlayer is

$$\gamma_{yz}(z,t) = -\frac{2}{rh} w_B(z,t) - \varphi(z,t) = -\left[\frac{2}{rh} w_C(z,t) + \frac{1+r}{r}\varphi(z,t)\right]. \tag{3.10}$$

But, since the fractional equation (3.3) remains valid, one obtains

$$\frac{\partial N(z,t)}{\partial z} = \frac{b}{r} C_\alpha \, {}_0^C\mathcal{D}_t^\alpha \left[\frac{2}{h} w_C(z,\cdot) + (1+r)\varphi(z,\cdot)\right](t)\,, \tag{3.11}$$

and, from this,

$$\frac{\partial^2 N(z,t)}{\partial z^2} = \frac{b}{rE} C_\alpha \, {}_0^C\mathcal{D}_t^\alpha \left[\frac{2}{hA} N(z,\cdot) + (1+r)\frac{M(z,\cdot)}{I}\right](t)\,. \tag{3.12}$$

With a few calculations, the governing fractional differential equations in terms of the displacement field $v(z,t)$ and the axial force $N(z,t)$, result to be of the form

$$\frac{\partial^4 v(z,t)}{\partial z^4} + \frac{(1+r)h}{2EI}\frac{\partial^2 N(z,t)}{\partial z^2} = \frac{p(z,t)}{2EI}\,, \tag{3.13}$$

$$\frac{\partial^2 N(z,t)}{\partial z^2} - \frac{2b}{rhEA} C_\alpha \, {}_0^C\mathcal{D}_t^\alpha [N(z,\cdot)](t) = -\frac{(1+r)b}{r} C_\alpha \, {}_0^C\mathcal{D}_t^\alpha \left[\frac{\partial^2 v(z,\cdot)}{\partial z^2}\right](t). \tag{3.14}$$

Four boundary conditions in z are requested in terms of $v(z,t)$ and two conditions in terms of $N(z,t)$. These shall be selected among the following.

$$v(z,t)\big|_{\substack{z=0\\z=L}} = \overline{v}(z,t)\big|_{\substack{z=0\\z=L}} \,, \tag{3.15a}$$

$$\left.\frac{\partial v(z,t)}{\partial z}\right|_{\substack{z=0\\z=L}} = -\overline{\varphi}(z,t)\big|_{\substack{z=0\\z=L}} \,, \tag{3.15b}$$

$$\left.\frac{\partial^2 v(z,t)}{\partial z^2}\right|_{\substack{z=0\\z=L}} = -\frac{1}{EI}\,\overline{M}(z,t)\big|_{\substack{z=0\\z=L}} \,, \tag{3.15c}$$

$$\left.\frac{\partial^3 v(z,t)}{\partial z^3}\right|_{\substack{z=0\\z=L}} = -\frac{1}{EI}\left[\overline{T}(z,t) + \frac{h}{2}\frac{\partial N(z,t)}{\partial z}\right]_{\substack{z=0\\z=L}} \,, \tag{3.15d}$$

$$N(z,t)\big|_{\substack{z=0\\z=L}} = \overline{N}(z,t)\big|_{\substack{z=0\\z=L}} \,, \tag{3.15e}$$

$$\left.\frac{\partial N(z,t)}{\partial z}\right|_{\substack{z=0\\z=L}} = -\overline{n}(z,t)\big|_{\substack{z=0\\z=L}} \,. \tag{3.15f}$$

Conditions (3.15a) to (3.15c) are standard for Euler-Bernoulli beam theory. Conditions (3.15e) and (3.15f) state that the values of the axial force, as well as its gradient with respect to z, in the upper beam (and correspondingly the antisymmetric value on the lower beam) may be prescribed. With regard to the gradient condition, recall from (3.2a) that $\frac{\partial}{\partial z}N(z,t)|_{z=0,L} = -b\tau_{yz}(z,t)|_{z=0,L}$: assigning the value of the $z-$gradient of N is equivalent to prescribing the shear force in the interlayer at the boundary during the load history. In particular, if the beam ends are prevented to slide one with respect to the other by an internal constraint placed at, say, $z = 0$, then $\gamma_{yz}(0,t) = 0$ and, consequently $-b\tau_{yz}(0,t) = \frac{\partial}{\partial z}N(z,t)|_{z=0} = 0$. In other words, this condition is in general explicated by an internal edge-constraint. Passing to (3.15d) observe that, at the boundary, the value of the $z-$gradient of order three of the displacement field is affected not only by an applied transversal force, but also by the shear stress transmitted by the interlayer.

In the particular case in which the structure is statically determined, so that the total bending moment $M_{\text{tot}}(z,t)$ acting at each composite cross section can be readily found as a function of the applied loads $p(z,t)$, the system of equations (3.13)-(3.14)

results to be uncoupled since (3.14) can be expressed as a function of $N(z,t)$ only. In fact, one can write

$$M_{\rm tot}(z,t) = 2M(z,t) - (1+r)hN(z,t)\,. \tag{3.16}$$

Solving for $M(z,t)$ and inserting the resulting expression in (3.12), the counterpart of (3.14) becomes

$$\frac{\partial^2 N(z,t)}{\partial z^2} - \frac{b}{rE}\frac{2I+(1+r)^2h^2A/2}{hAI}C_\alpha\ {}_0^C\mathcal{D}_t^\alpha[N(z,\cdot)](t) = \frac{(1+r)b}{2rEI}C_\alpha\ {}_0^C\mathcal{D}_t^\alpha[M_{\rm tot}(z,\cdot)](t)\,, \tag{3.17}$$

with boundary conditions (3.15e)-(3.15f). An argument of this type seems to have been first used by Newmark [48] while considering the compliant shear coupling provided by elastic stud connectors between the concrete slab and steel beams in hybrid steel-concrete structures. Once $N(z,t)$ has been determined, the field $v(z,t)$ can be found from (3.13).

Observe in (3.17) that the quantity $2I+(1+r)^2h^2A/2 = I_M$ is the moment of inertia of a cross section composed of two $b\times h$ rectangles spaced of rh. The *monolithic limit* corresponds to the case of rigid coupling of the glass plies through the interlayer (negligible shear in the polymer), so that the laminate responds to bending as a monolith with cross-sectional inertia I_M. The opposite case is that of the *layered limit*, when the glass plies can freely slide with negligible shear coupling: the effective cross-sectional moment of inertia is clearly $I_L = 2I$.

It is interesting to consider the response predicted by the governing equations (3.13) and (3.14) at such borderline cases when no axial force is introduced at the laminate ends, i.e., $\overline{N}(0,t) = \overline{N}(L,t) = 0$ in (3.15e). The *layered limit* is attained when $C_\alpha \to 0$

in (3.3) or, equivalently, $r \to \infty$. Then, (3.14) reduces to $\frac{\partial^2}{\partial z^2} N(z,t) = 0$ and, from the aforementioned boundary conditions, one obtains $N(z,t) = 0$. With this condition, (3.13) provides the classical equation $EI_L \frac{\partial^4}{\partial z^4} v(z,t) = p(z,t)$.

When $C_\alpha \to \infty$ or $r \to 0$, as in the *monolithic limit*, (3.14) gives

$$\frac{2}{hEA} \, {}_0^C\mathcal{D}_t^\alpha [N(z,\cdot)](t) = (1+r) \, {}_0^C\mathcal{D}_t^\alpha \left[\frac{\partial^2 v(z,\cdot)}{\partial z^2} \right](t). \tag{3.18}$$

This implies that $N(z,t) = \frac{1}{2}(1+r)hEA \frac{\partial^2}{\partial z^2} v(z,t) + g(z)$, where $g(z)$ is an unknown function of the only variable z but, clearly, for a quiescent system $g(z) = 0$. Substituting in (3.13) and recalling that $I_M = 2I + (1+r)^2 h^2 A/2$, one readily obtains $EI_M \frac{\partial^4}{\partial z^4} v(z,t) = p(z,t)$.

Solutions for the intermediate case $0 < C_\alpha < \infty$ will be discussed in the following Sections.

4. Step-by-step solution

Referring to the simply supported beam of Figure (1), let $p(z,t)$ represent a *quasi-static* time-varying loading load history, in the sense that it induces negligible accelerations and, consequently, negligible inertial actions. Suppose that no normal forces are applied at the laminate ends and that the glass plies can freely slide one another. From (3.15), the boundary conditions are

$$v(0,t) = 0\,, \;\; v(L,t) = 0\,, \tag{4.1a}$$

$$\left.\frac{\partial^2 v(z,t)}{\partial z^2}\right|_{z=0} = 0\,, \quad \left.\frac{\partial^2 v(z,t)}{\partial z^2}\right|_{z=L} = 0\,, \tag{4.1b}$$

$$N(0,t) = 0\,, \;\; N(L,t) = 0\,. \tag{4.1c}$$

Since the structure is statically determined, $M_{\rm tot}(z,t)$ can be readily calculated in terms of $p(z,t)$ and, consequently, one can find $N(z,t)$ from (3.17).

The step-by-step solution technique of the fractional differential equation is proposed under the hypothesis that $p(z,t)$ is *continuous* with its time derivative on the whole temporal axis $[0,\mathcal{T})$, being $\mathcal{T}$ the final time of observation. Because of (4.1c) and since, from (4.1b), $M_{\rm tot}(0,t) = M_{\rm tot}(L,t) = 0$, $\forall t \in [0,\mathcal{T})$, both $N(z,t)$ and $M_{\rm tot}(z,t)$ can be expanded in Fourier series with even terms according to

$$N(z,t) = \sum_{k=1}^{\infty} N_k(t) \sin\left(k\pi z/L\right) \,, \tag{4.2a}$$

$$M_{\rm tot}(z,t) = \sum_{k=1}^{\infty} M_k(t) \sin\left(k\pi z/L\right) \,. \tag{4.2b}$$

The equation (3.17) can be re-written as

$$\frac{\partial^2 N(z,t)}{\partial z^2} - Q_\alpha \, {}_0^C\mathcal{D}_t^\alpha[N(z,\cdot)](t) = P_\alpha \, {}_0^C\mathcal{D}_t^\alpha[M_{\rm tot}(z,\cdot)](t) \,, \tag{4.3}$$

where

$$Q_\alpha = C_\alpha \frac{b}{rE} \frac{4I + (1+r)^2 h^2 A}{2hAI} \,, \quad P_\alpha = C_\alpha \frac{(1+r)b}{2rEI} \,. \tag{4.4}$$

By inserting (4.2) in (4.3), multiplying both members of the resulting equation by $\sin(k\pi z/L)$ and integrating for $z \in (0,L)$, the following fractional differential equation in the unknowns $N_k(t)$ is readily found

$${}_0^C\mathcal{D}_t^\alpha[N_k(\cdot)](t) + \Lambda_k^{(\alpha)} N_k(t) = -R_\alpha \, {}_0^C\mathcal{D}_t^\alpha[M_k(\cdot)](t) \,, \quad k = 1, 2 \ldots \tag{4.5}$$

with

$$\Lambda_k^{(\alpha)} = \frac{k^2\pi^2}{L^2 Q_\alpha}\,, \quad R_\alpha = \frac{P_\alpha}{Q_\alpha}\,. \tag{4.6}$$

Equations (4.5) constitute a set of decoupled fractional differential equations. Because of the regularity assumptions on $p(z,t)$ and, hence, on $M_{\rm tot}(z,t)$, the Grünwald-Letnikov (GL) integration scheme can be used to evaluate $N_k(t)$. This consists in the discretization of the interval $[0,T]$ into s small intervals of amplitude $\Delta t = t_j - t_{j-1}$, $j = 1 \dots s$, being t_j the subdivision times. Moreover, the $s-$vectors $\mathbf{N}_{k,s}$ and $\mathbf{M}_{k,s}$ are defined, whose $j-$th component are $N_k(t_j)$ and $M_k(t_j)$, i.e.,

$$\mathbf{N}_{k,s}^T = [N_k(t_1), N_k(t_2) \dots N_k(t_s)]\,, \quad \mathbf{M}_{k,s}^T = [M_k(t_1), M_k(t_2) \dots M_k(t_s)]\,. \tag{4.7}$$

By following the GL step-by-step integration scheme, the fractional derivatives of $N_k(t)$ and $M_k(t)$, evaluated at the time instants $t_1, t_2 \dots t_s$, may be written as

$$\boldsymbol{\nabla}^\alpha_{GL,s} N_k(t) = \mathbf{A}^{(\alpha)}_{k,s} \mathbf{N}_{k,s}\,, \quad \boldsymbol{\nabla}^\alpha_{GL,s} M_k(t) = \mathbf{A}^{(\alpha)}_{k,s} \mathbf{M}_{k,s}\,, \tag{4.8}$$

where the symbols $\boldsymbol{\nabla}^\alpha_{GL,s} N_k(t)$ and $\boldsymbol{\nabla}^\alpha_{GL,s} M_k(t)$ denote vectors whose components are the fractional derivatives of $N_k(t)$ and $M_k(t)$ evaluated at the time instants $t_1, t_2 \dots t_s$. In (4.8) the $s \times s$ matrix $\mathbf{A}^{(\alpha)}_{k,s}$ is a lower band strip matrix defined as

$$\mathbf{A}^{(\alpha)}_{k,s} = \frac{1}{(\Delta t)^\alpha} \begin{bmatrix} \omega_1(\alpha) & & & \\ \omega_2(\alpha) & \omega_1(\alpha) & & \\ \vdots & \ddots & \ddots & \\ \omega_s(\alpha) & \cdots & \omega_2(\alpha) & \omega_1(\alpha) \end{bmatrix}\,, \tag{4.9}$$

and the coefficients $\omega_j(\alpha)$, $j = 1 \dots s$, can be evaluated recursively, as

$$\omega_1 = 1,\ \omega_2 = -\alpha, \ldots, \omega_{j+1}(\alpha) = \frac{j-\alpha-1}{j}\omega_j(\alpha)\,. \tag{4.10}$$

The GL approach leads to a fully consistent step-by-step procedure for evaluating the fractional derivatives and integrals as, in fact, the basic rules of ordinary derivative and integrals still hold.

By inserting eqs (4.8) into (4.5), one obtains

$$\left(\mathbf{A}_{k,s}^{(\alpha)} + \Lambda_{k,s}^{(\alpha)}\mathbf{I}_s\right)\mathbf{N}_{k,s} = -R_\alpha \mathbf{A}_{k,s}^{(\alpha)}\mathbf{M}_{k,s}\,, \tag{4.11}$$

where $\mathbf{I}_s$ is the $s \times s$ identity matrix.

Therefore, once the bending moment is known, $\mathbf{N}_{k,s}$ is given by

$$\mathbf{N}_{k,s} = -R_\alpha \mathbf{B}_{k,s}^{(\alpha)}\mathbf{A}_{k,s}^{(\alpha)}\mathbf{M}_{k,s}\,, \tag{4.12}$$

where $\mathbf{B}_{k,s}^{(\alpha)}$ is given by

$$\mathbf{B}_{k,s}^{(\alpha)} = \left(\mathbf{A}_{k,s}^{(\alpha)} + \Lambda_{k,s}^{(\alpha)}\mathbf{I}_s\right)^{-1}\,. \tag{4.13}$$

From (4.12) it seems that to calculte the response at each new time instant t_{s+1} one needs to evaluate the inverse of the matrix $\mathbf{A}_{k,s}^{(\alpha)} + \Lambda_{k,s}^{(\alpha)}\mathbf{I}_s$, requiring $1^3 + 2^3 + \cdots + s^3 + (s+1)^3$ products. However, since the sum of lower band strip matrices is a lower band strip matrix, and the inverse of a lower band strip matrix is still a lower band strip matrix, it follows the entire $\mathbf{B}_{k,s}^{(\alpha)}$ is fully described by the elements of the first column (or the last row) and these entries may be easily evaluated in recursive form as follows. Let $\mathbf{U}_s$ be a lower band strip matrix and denote with $\mathbf{V}_s$ its inverse, i.e., $\mathbf{U}_s\mathbf{V}_s = \mathbf{I}_s$. The first column of $\mathbf{V}_s$ is correlated with the first column of $\mathbf{U}_s$ by

$$V_1 = \frac{1}{U_1}\,, \quad V_2 = -\frac{1}{U_1} U_2 V_1\,, \quad V_s = -\frac{1}{U_1}\left(\sum_{j=1}^{s-1} V_j U_{s+1-j}\right)\,. \tag{4.14}$$

Once $V_1, V_2, \ldots, V_s$ have been evaluated, the entire matrix can be easily constructed, with limited computational effort.

5. Applications

After a discussion on the calibration of the material parameters that are needed to define the fractional viscoelastic model, this is applied in explanatory examples.

5.1. Calibration of material parameters

The material parameters that are needed for the fractional viscoelastic characterization of the polymeric interlayer, as per (2.3), or equivalently (2.8), are the exponent α and the coefficient C_α. These can be directly calculated from (2.1), once the creep function $G(t)$ has been experimentally evaluated, or from (2.7), if the relaxation function $R(t)$ is measured. Recall that the fractional viscoelastic model, in agreement with experiments [24], prescribes a power-law response in terms of creep and relaxation.

For the calibration, reference is made to the careful experimental campaign conducted by Biolzi et al [11], who tested polymeric films of polyvinyl butyral (PVB), ionoplast SentryGlas (SG) and high performance plasticized PVB (commercially known as DG41 and referred to as DG). There are obviously many types of polymers, each characterized by a peculiar response, but this work focuses on laminated glass for which the above materials are the most commonly used as interlayers. The experimental apparatus was designed to apply a displacement on the central glass ply of a three-ply laminated glass specimen, while the external plies are held fixed. In this way, similarly to shear tests on bolted double-lap joints of steel elements, the two

polymeric interlayers forming the laminated packages are approximately subjected to a uniform shear strain. Using a load cell or a dynamometric ring, one can measure the resultant of the shear stresses on the central ply. Experiments were conducted in a climatic chamber at various temperatures, ranging from 10° C to 50° C. The relaxation function was obtained by keeping the shear strain constant (within the experimental tolerances) and measuring the resultant of the shear stresses, assuming that these are homogeneously and uniformly distributed in the polymer-glass interfaces. The creep function was conventionally measured under the hypothesis of linear viscoelastic response during the unloading phases. Direct measurements were conducted on time intervals of the order on one day and were extrapolated over longer time intervals by using the time-temperature superposition principle according to the Williams Landel Ferry equation [20].

The experimental points that are here used refer to the direct observation of the relaxation function, which represents the datum obtained from direct objective measures. For all the three considered materials (SG, DG, PVB), representative experimental graphs of the relaxation function $R(t)$ obtained at various temperatures (indicated in °C in the labels) are reported in Figure 5 as a function of time. Remarkably, for temperatures ranges away from the glass-transition temperature of the polymer and outside the branch of the curve that corresponds to it according to the Williams Landel Ferry model [20], the graphs can be well-approximated by a power-law of the form (2.7), which corresponds to a linear trend in the bi-logarithmic plane. The corresponding best fit interpolation, with the corresponding equation, is also reported in the same picture.

For the power-laws so obtained, it is immediate to calculate the parameter α and C_α from (2.7). The corresponding values are collected in Table 1

It should be observed that, in the classical approach, it is customary to approximate

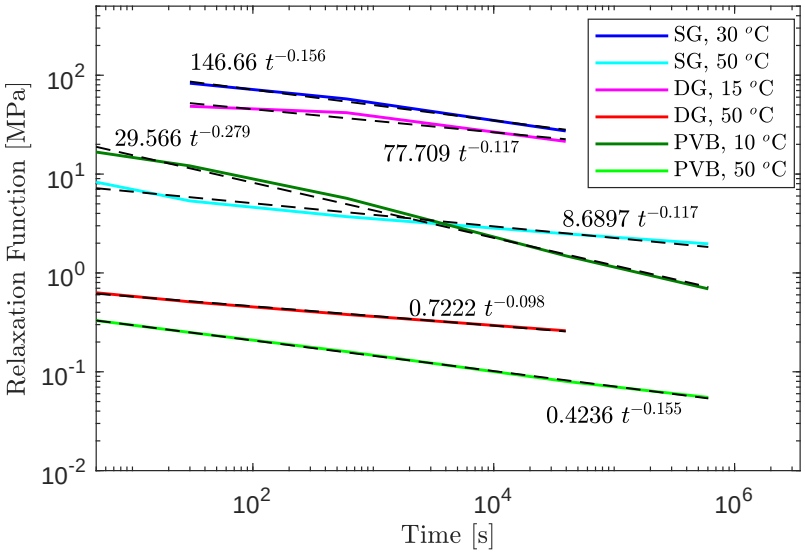

Figure 5: Relaxation fuction for three polymeric interlayers (SG, DG, PVB) at various temperatures (indicated in °C in the labels), obtained from the experimental campaign of [11]. Interpolation with a power law (linear trend in the bi-log plane) and corresponding expressions.

Table 1: Fractional viscoelastic parameters α and C_α for three polymeric interlayers (SG, DG, PVB) at various temperatures, calibrated from the experimental campaign of [11].

Material	Temp. [° C]	α	C_α [MPa s$^{-\alpha}$]
SG	30	0.156	146.66
SG	50	0.117	8.6897
DG	15	0.117	77.709
DG	50	0.098	0.7222
PVB	10	0.279	29.566
PVB	50	0.155	0.4236

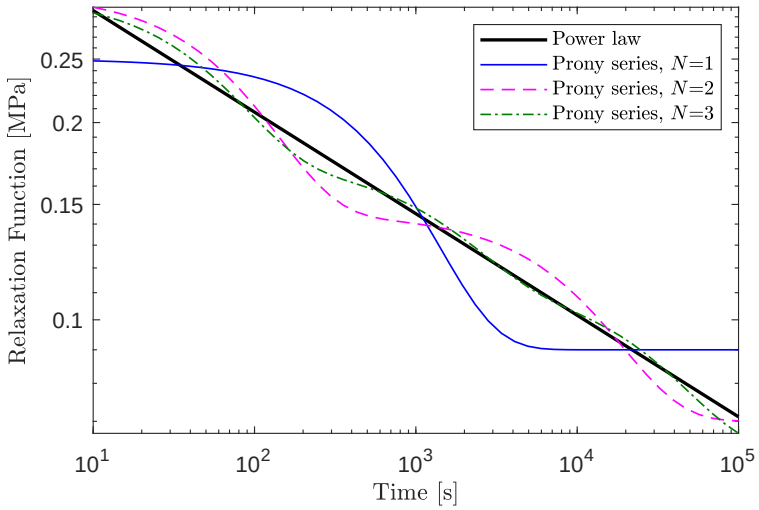

Figure 6: Interpolation of the power law relaxation function for PVB 50 with Prony series with 1, 2 and 3 exponential terms.

the relaxation function or, equivalently, the creep function, with the sum of decaying exponential functions, referred to as Prony's series, of the form

$$R(t) = R_0 + \sum_{j=1}^{N} R_i \exp[-t/\tau_j]\,, \tag{5.1}$$

where R_0 represents the steady state, R_j are the modulus terms and τ_j the relaxation times, respectively. This represents the response of a generalized Maxwell model, also known as the Wiechert model, which is composed by one elastic spring and N spring-dashpot Maxwell elements. The number N needs to be high in order to interpret with sufficient accuracy the experimental results. With reference to the PVB 50 represented in Figure 5, the approximation of the corresponding power-law curve (labelled "power" in the picture) that can be obtained with $N = 1, 2, 3$ is evidenced by the graphs in Figure 6. The Prony series regression has been obtained with the Domain Of Influence (DOI) method proposed in [21].

The graph corresponding to $N = 1$ evidences the peculiarities of the exponential function. The slope of the relaxation curve is small for most of the considered time and, therefore, it contributes very little to the series [21]; quite a sharp decay is evident only in a neighborhood of the relaxation time τ_1. In conclusion, the power law trend, characteristic of the actual material response, can be interpolated with very poor accuracy. Increasing the number of terms, with $N = 2$ and $N = 3$ a better accuracy can be obtained, but the interpolating curve always presents "jumps" at the corresponding relaxation times. In other words, a Prony series approximates a power-law response not uniformly, but with a "hopping" trend. It should also be recalled that if one needed to capture the viscoelastic response for extremely short times, as in the case of impulsive loadings, in order to define the relaxation time of the corresponding exponential term in the Prony's series it would be necessary to conduct careful experiments on a time-scale of the same order, with remarkable difficulties. This problem is by-passed if one directly handles the power-law response with the mathematical tool of fractional calculus.

It should be noted, however, that the proposed experimental data refer to a limited observation period, of the order of one day. Extrapolation to longer periods is generally performed according to the"time-temperature superposition principle", usually (at least in glass engineering) based upon Williams-Landel-Ferry theory [20], which postulates a dilatation of the characteristic time-scale as a function of the temperature. Thus, it is possible to trade off temperature for time and conduct short-term experiments at different temperatures to evaluate the response over time spanning many decades [49]. Short-term tests in a neighborhood of the glass transition temperature exhibit a noteworthy deviation from the simple power-law response which, according to this rationale, should be associated with long-term relaxations. At this stage, the power-law cannot fit any more the experimental data and, therefore, the simplest fractional viscoelastic model, based on two parameters, cannot be consis-

tently applied. This scenario could be considered with more refined models [50] [51] of fractional viscoelasticity, but this is beyond the scope of the present article, which is focused on the response of laminated glass under moderately varying actions, far from the glass transition temperature of the polymer.

5.2. Numerical experiments

In order to illustrate the potential of the fractional viscoelastic characterization, it is convenient to refer to the simplest case in which the beam of Figure 1 is subjected to forces per unit length sinusoidally distributed that provide a sinusoidal bending moment, i.e.,

$$p(z,t) = \overline{p}(t)\sin\left(\pi z/L\right)\ , \quad M_{\rm tot}(z,t) = \frac{L^2}{\pi^2}\overline{p}(t)\sin\left(\pi z/L\right)\ . \tag{5.2}$$

Since the only surviving terms in (4.5) are those corresponding to $k=1$, this equation becomes

$$ {}_0^C\mathcal{D}_t^\alpha[N_1(\cdot)](t) + \Lambda_1^{(\alpha)} N_1(t) = -R_\alpha \frac{L^2}{\pi^2}\, {}_0^C\mathcal{D}_t^\alpha[\overline{p}(\cdot)](t)\,. \tag{5.3}$$

Once $N_1(t)$, and hence $N(z,t)$, have been determined, the displacement field $v(z,t)$ can be found from (3.13), which becomes

$$v(z,t) = v_1(t)\sin\left(\pi z/L\right) \quad \text{with} \quad v_1(t) = \left[\overline{p}(t) + \frac{\pi^2(1+r)h}{L^2}N_1(t)\right]\frac{L^4}{2\pi^4 EI}\,. \tag{5.4}$$

Observe, here, that the form of $N_1(t)$ is in general different from that of $\overline{p}(t)$. This provokes the shifting of the response of the laminate in terms of displacement with respect to the applied actions.

It is useful to consider the monolithic limit for $C_\alpha \to \infty$. Reasoning as indicated at the end of Section 3, one obtains

$$N_M(z,t) = -\frac{(1+r)hA}{2I_M} M_{\rm tot}(z,t) = N_{1,M}(t)\sin(\pi z/L)\,, \tag{5.5a}$$

$$N_{1,M}(t) = -\frac{L^2}{\pi^2}\frac{(1+r)hA}{2I_M}\overline{p}(t)\,, \tag{5.5b}$$

so that, from (5.5), $v_1(t) = \overline{p}(t)L^4/(\pi^4 E I_M)$.

The geometric parameters that will be considered in the following are $h = 10\,\mathrm{mm}$, $b = 1\,\mathrm{m}$, $L = 3\,\mathrm{m}$, $r = 0.152$, $A = b \times h$, $I = \frac{1}{12}bh^3$, $E = 70\,\mathrm{GPa}$. Various forms for $\overline{p}(t)$ will be discussed in the sequel.

5.2.1. Harmonic excitation

The harmonic excitation of the laminate corresponds to the case in which (5.2) reads

$$\overline{p}(t) = p_0 \sin(\Omega t) = p_0 \sin(2\pi t/T)\,. \tag{5.6}$$

Setting $p_0 = 0.5\,\mathrm{kN/m}$, consider first the case in which the period T is quite long, i.e., $T = 5 \times 10^3\,\mathrm{s}$. For $C_\alpha = 131.151\,\mathrm{MPa\,s^{-\alpha}}$, close[1] to the greatest measured value in Table 1, Figure 7 reports the graphs of the function $N_1(t)$ in the interval $0 \le t \le 2\,T$ for various values of the exponent $\alpha \in (0,1)$ and, for the sake of comparison, the value $N_{1,M}(t)$ as per (5.5b), corresponding to the monolithic limit.

In order to interpret the results, notice that when $\alpha \to 0$, the interlayer becomes linear elastic, with shear modulus $G = C_0 = 131.151\,\mathrm{MPa}$. In fact, in (2.9) $\Gamma(1) = 1$

[1]This value has been selected by considering the mean of comparable tests in [11].

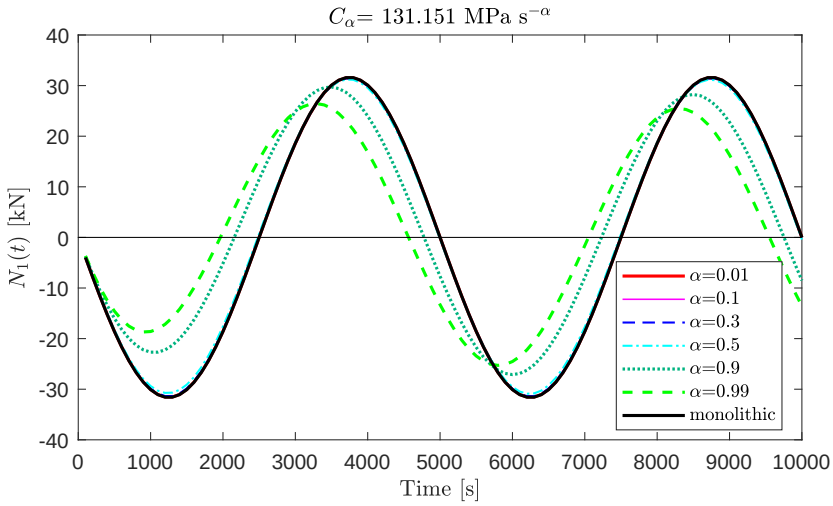

Figure 7: Graphs of the function $N_1(t)$ [kN] as a function of time t [s] for $T = 5 \times 10^3$ s, $C_\alpha = 131.151$ MPa s$^{-\alpha}$ and various values of α and comparison with the monolithic case.

and, from (2.8), one obtains $\tau(t) = C_0\gamma(t)$. On the other hand, when $\alpha \to 1$, the response is purely viscous (simple dashpot) with constant $\mu = C_1 = 131.151\,\text{MPa}\,\text{s}^{-1}$, because, from (2.3) and (2.4), one has

$$\gamma(t) = \frac{1}{C_1}\int_0^t \tau(\bar{t})\,d\bar{t} \quad \Rightarrow \quad \tau(t) = C_1\dot{\gamma}(t)\,. \tag{5.7}$$

Under a slow oscillating action, the response of the laminate coincides in practice with the monolithic limit when $\alpha < 0.5$: in this case, the elastic component of the viscoelastic response of the interlayer plays a decisive role. For higher values of α the response tends to be purely viscous and, hence, the coupling between the glass plies diminishes.

This trend can be better appreciated in the graphs of Figure 8 corresponding to $C_\alpha = 0.379\,\text{MPa}\,\text{s}^{-\alpha}$, approaching the lower value in Table 1. The graph closer to the monolithic limit is that corresponding to $\alpha \simeq 0.01$, because of the elastic contribution. However, the coupling between the glass plies diminishes as α is augmented. In

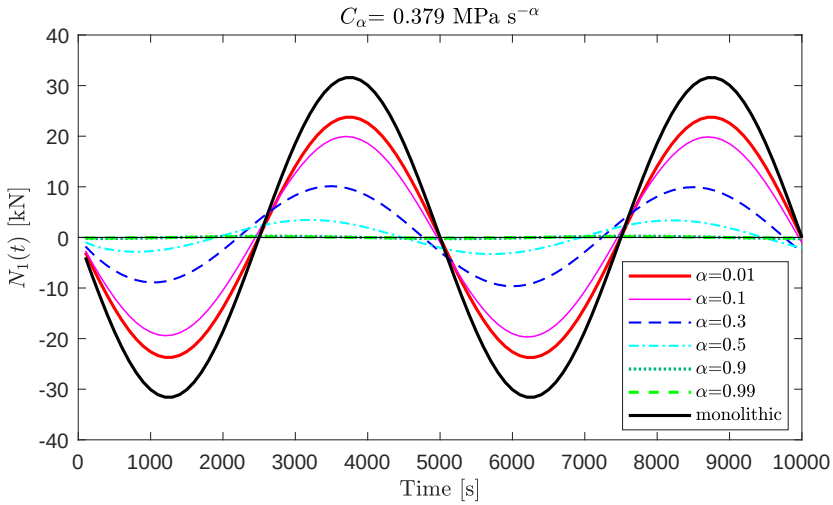

Figure 8: Graphs of the function $N_1(t)$ [kN] as a function of time t [s] for $T = 5 \times 10^3$ s, $C_\alpha = 0.379\,\mathrm{MPa\,s^{-\alpha}}$, various values of α and comparison with the monolithic case.

practice, $N_1(t)$ is null when $\alpha > 0.5$ because the viscosity constant is so small that, at the applied frequency, it cannot produce the shear coupling of the glass plies, which in practice are allowed to freely slide one on the other (layered limit).

By decreasing the period of the applied load to $T = 5$ s, the response in terms of $N_1(t)$ becomes that represented in Figures 9 and 10, which are the counterparts of Figures 7 and 8, respectively.

It is clear from Figure 9 that for the high value of C_α all graphs overlap on the monolithic case. In fact, when the oscillations are relatively fast, either the elastic or the viscous component of the interlayer response are sufficient to assure the perfect coupling of the glass plies.

If the coefficient C_α is reduced, the coupling is consequently diminished. For $\alpha = 0.01$, the response is in practice equivalent to that of Figure 8: when the response is purely elastic, the influence of the frequency of the applied force is negligible. On the other hand, increasing α the coupling associated with the viscoelastic part is sensibly higher,

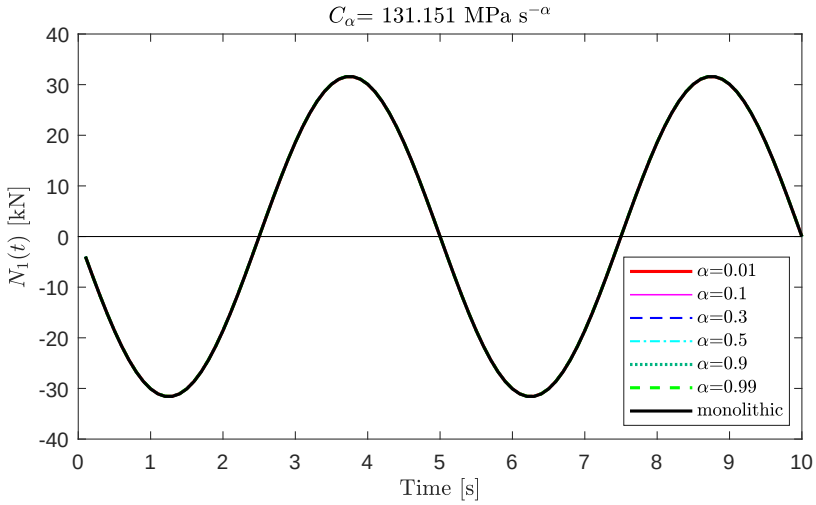

Figure 9: Graphs of the function $N_1(t)$ [kN] as a function of time t [s] for $T = 5\,\mathrm{s}$, $C_\alpha = 131.151\ \mathrm{MPa\,s}^{-\alpha}$, various values of α and comparison with the monolithic case.

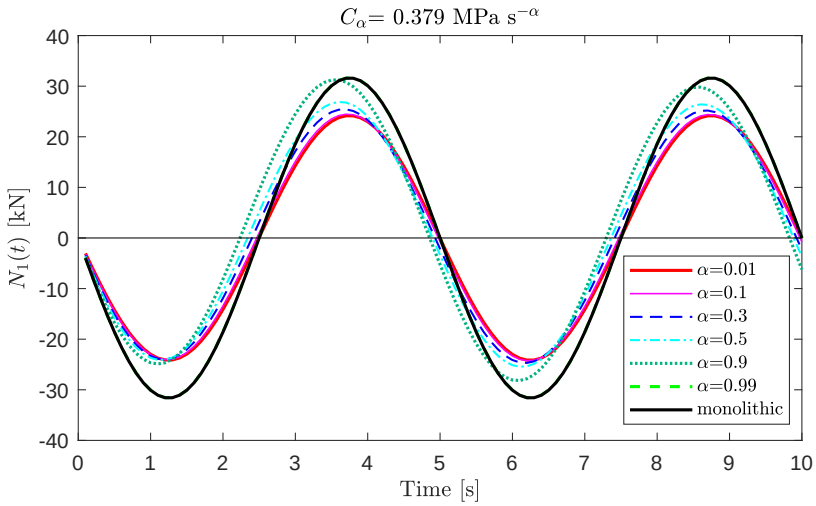

Figure 10: Graphs of the function $N_1(t)$ [kN] as a function of time t [s] for $T = 5\,\mathrm{s}$, $C_\alpha = 0.379\ \mathrm{MPa\,s}^{-\alpha}$, various values of α and comparison with the monolithic case.

because now the frequency of the forcing load plays a decisive role.

5.2.2. Pseudo-constant load

The present approach can be applied only if the applied load is a continuous function of time starting from the null value. In order to approximate the application of a constant load, which would be rigorously defined by a step function, consider in (5.2) a law of the type

$$\overline{p}(t) = p_0 \left(1 - e^{-t/t_0}\right) , \tag{5.8}$$

which tends to p_0 for $t \to \infty$ and remains almost constant from $t \gg t_0$. In the following reference will be made to the case $t_0 = 2\,\mathrm{s}$ and $p_0 = 0.5\,\mathrm{kN/m}$, for an observation time $\mathcal{T} = 20\,t_0$.

For $C_\alpha = 131.151\,\mathrm{MPa\,s^{-\alpha}}$, the graphs of $N_1(t)$ for varying α are reported in Figure 11. With this datum, the laminate response is close to the monolithic limit. The effect of viscosity is that of producing a reduction (in absolute value) of $N_1(t)$, and hence of the shear coupling, with time, proportionally to increasing α.

The viscoleastic properties can be better appreciated in Figure 12, corresponding to the case $C_\alpha = 0.379\,\mathrm{MPa\,s^{-\alpha}}$. The monolithic limit is never attained and the condition that better approaches this borderline case is that with $\alpha = 0.01$. Since this case is similar to that of a purely elastic polymer, $N_1(t)$ does not exhibit a noteworthy decay, at least in the time of observation. As α is augmented, the viscoelastic component tends to dominate the response. For $\alpha \geq 0.9$, the axial force $N_1(t)$ becomes almost null after a few seconds, the decay being the faster the higher is α.

Indeed, the strength of the fractional viscoelastic model is that only two parameters are needed to calibrate a power-law relaxation curve. On the other hand, the traditional approach for laminated glass based, upon series of Prony, usually requires

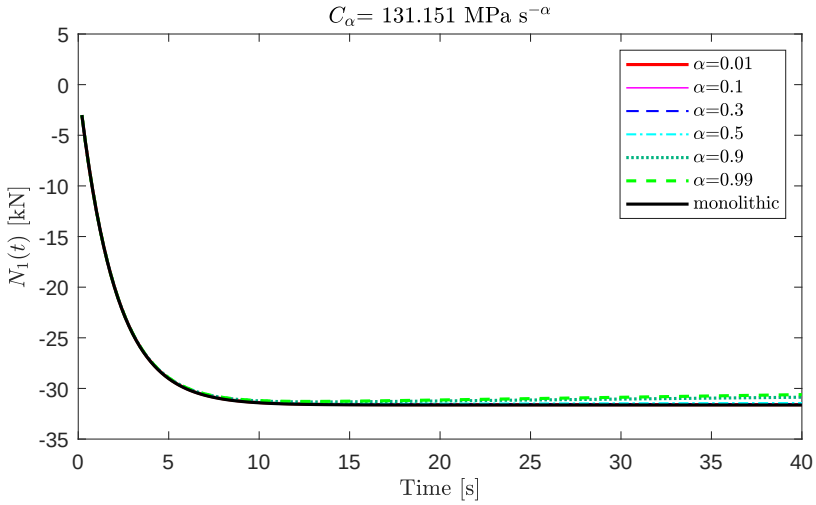

Figure 11: Graphs of the function $N_1(t)$ [kN] as a function of time t [s] for $t_0 = 2\,\mathrm{s}$, $p_0 = 0.5\,\mathrm{kN/m}$, $C_\alpha = 131.151\ \mathrm{MPa\,s}^{-\alpha}$, various values of α and comparison with the monolithic case.

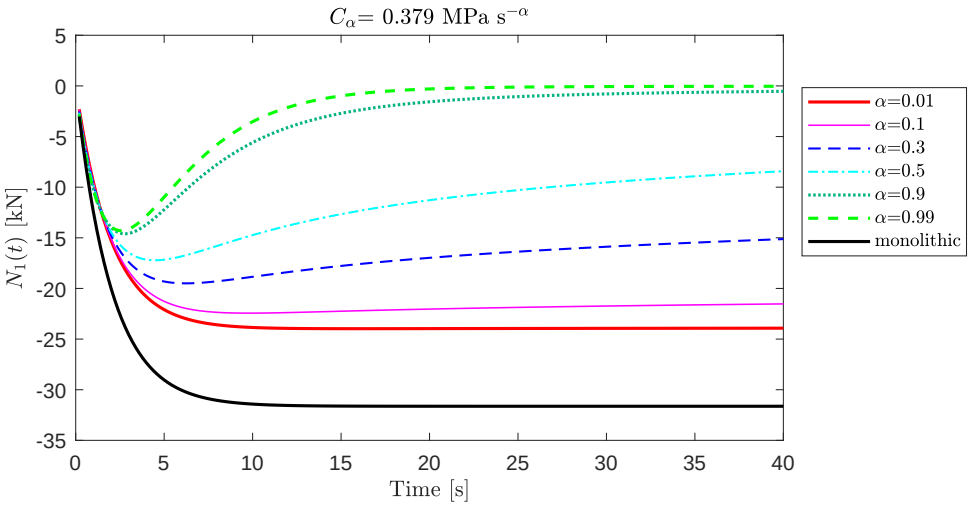

Figure 12: Graphs of the function $N_1(t)$ [kN] as a function of time t [s] for $t_0 = 2\,\mathrm{s}$, $p_0 = 0.5\,\mathrm{kN/m}$, $C_\alpha = 0.379\ \mathrm{MPa\,s}^{-\alpha}$, various values of α and comparison with the monolithic case.

$15-20$ terms, each characterized by 2 parameters, whose calibration is therefore quite difficult [21]. Of course, in the worked examples just presented, if such a large number of terms were used in the Prony's series, the response would become indistinguishable from that predicted by the fractional model. Under a pure harmonic loading, just those terms of the series directly associated with the frequency of the applied loads could be considered, but if the frequency is changed, other terms should be added. It is not easy to make a direct comparison between the two approaches (Prony and fractional), because this would require a sensitivity analysis based on the number of terms that are used in the series, and doing numerical experiments at varying frequencies. Furthermore, the coefficients of the Prony's series strongly vary according to the parameter α, corresponding to the exponent in the power-law dependence, which characterizes, per se, the wide variety of responses that can be expected in polymeric interlayers for laminated glass.

It is important to recall, however, that we are not claiming that the fractional viscoelastic model provides better results than the classical approach using series of Prony. We simply indicate that, in order to reproduce a dependence on the power law, the fractional approach requires a much lower number of parameters than the Prony approach and, therefore, calibration is facilitated.

6. Conclusions

The structural design of laminated glass requires effective models for the viscoelastic properties of the polymeric interlayer. These are of paramount importance, since it is from the polymer that the shear coupling of the glass layers is generated; this greatly influences the load-bearing capacity of the whole laminate. This article has illustrated the potential advantages of a fractional differential characterization of the viscoelastic response of the polymer. Reference has been made to the paradigmatic example of a three-layered symmetric laminated beam, composed by two glass plies

sandwiching a thin polymeric interlayer, where the possibility of zig-zag warping of the cross section is taken into account.

The deviatoric shear deformation of the polymeric interlayer has been correlated with the shear stress by a constitutive law defined via Caputo's fractional derivative, determined by only two material parameters. According to this rationale, the stress corresponding to a relaxation test (constant strain) exhibits a power-law dependence on time, which can fit with great accuracy the experimental measurements for polymers used in laminated glass, on representive time-scales and at arbitrary temperature, as long as this does not coincide with that of glass-transition. Hence, calibration of the fractional viscoelastic model is straightforward. On the other hand, the traditional design approach for laminated glass, which uses a Prony's series of units arranged according to the Maxwell-Wiechert model, necessitates of at least $10 - 15$ terms, for which the relaxation times shall span the whole time-scales of the applied actions. The Grünwald-Letnikov integration scheme has been used to evaluate the time history of the beam deflection under time-varying loading: this is easy to implement and requires a limited computational effort. In this article only the effects of quasi-static loading varying over time have been considered, neglecting the contribution of the inertial mass in order to simplify the equations and permit the analytical treatment. However, the extension to the dynamic case does not present conceptual difficulties.

The fact that a single fractional term can interpret the viscoelastic response for arbitrary (whatever small) characteristic-duration of the applied actions, allows to embrace, after calibration from slow relaxation tests, also the effects of exceptional impulsive actions such as those from a blast wave. More in general, it should be mentioned that the model presented here can accurately consider branches of the relaxation curve of the power-law type, but a generalization is needed in order to in-

terpret those branches associated with the glass transition of the polymer. In further work, this point could be investigated by interpolating the whole relaxation curve with just a few terms of a power-law series, each term of which shall be interpreted by one fractional viscoelastic unit of the same type presented here. The implementation of dedicated engineering software for the calculation of laminated glass, based on a fractional viscoelastic model, not only presents no additional difficulties compared to the traditional approaches based on the Prony's series but, indeed, it is much simpler.

Acknowledgement. This research has not been supported by any specific grant from funding agencies in the public, commercial or not-for-profit sectors.

References

[1] Hooper J. On the bending of architectural laminated glass. International Journal of Mechanical Sciences 1973;15(4):309–23.

[2] Galuppi L, Royer-Carfagni G. A homogenized analysis á la Hashin for cracked laminates under equi-biaxial stress. Applications to laminated glass. Composites Part B: Engineering 2017;111:332–47.

[3] Ivanov I. Analysis, modelling, and optimization of laminated glasses as plane beam. International Journal of Solids and Structures 2006;43(22-23):6887–907.

[4] Kuntsche J, Schuster M, Schneider J. Engineering design of laminated safety glass considering the shear coupling: a review. Glass Structures and Engineering 2019;4(2):209–28.

[5] Eisenträger J, Naumenko K, Altenbach H, Köppe H. Application of the first-order shear deformation theory to the analysis of laminated glasses and photovoltaic panels. International Journal of Mechanical Sciences 2015;96-97:163–71.

[6] Amabili M, Balasubramanian P, Garziera R, Royer-Carfagni G. Blast loads and nonlinear vibrations of laminated glass plates in an enhanced shear deformation theory. Composite Structures 2020;252:art.112720.

[7] Galuppi L, Royer-Carfagni G. Effective thickness of laminated glass beam. New expression via variational approach. Eng Struct 2012;38:53–67.

[8] Galuppi L, Royer-Carfagni G. The effective thickness of laminated glass plates. J Mech Mat Struct 2012;7:375–400.

[9] Bardella L, Paterlini L, Leronni A. Accurate modelling of the linear elastic flexure of composite beams warped by midlayer slip, with emphasis on concrete-timber systems. International Journal of Mechanical Sciences 2014;87:268–80.

[10] Martín M, Centelles X, Solé A, Barreneche C, Fernández AI, Cabeza LF. Polymeric interlayer materials for laminated glass: A review. Construction and Building Materials 2020;230:art. 116897.

[11] Biolzi L, Cattaneo S, Orlando M, Piscitelli L, Spinelli P. Constitutive relationships of different interlayer materials for laminated glass. Composite Structures 2020;244:art. 112221.

[12] Schapery R. A method of viscoelastic stress analysis using elastic solutions. Journal of the Franklin Institute 1965;279(4):268–89.

[13] Galuppi L, Royer-Carfagni G. Laminated beams with viscoelastic interlayer. International Journal of Solids and Structures 2012;49(18):2637–45.

[14] Zemanová A, Zeman J, Šejnoha M. Comparison of viscoelastic finite element models for laminated glass beams. International Journal of Mechanical Sciences 2017;131-132:380–95.

[15] Galuppi L, Royer-Carfagni G. The design of laminated glass under time-dependent loading. International Journal of Mechanical Sciences 2013;68:67 – 75.

[16] Bennison S, Jagota A, Smith C. Fracture of glass/polyvinyl butyral (butacite) laminates in biaxial flexure. J Am Ceram Soc 1999;82(7):1761–70.

[17] Van Duser A, Jagota A, Bennison S. Analysis of glass/polyvinyl butyral laminates subjected to uniform pressure. Journal of Engineering Mechanics 1999;125(4):435–42.

[18] Wiechert E. Gesetze der elastischen Nachwirkung für constante Temperatur. Annalen der Physik 1893;286(11):546–70.

[19] Andreozzi L, Briccoli Bati S, Fagone M, Ranocchiai G, Zulli F. Dynamic torsion tests to characterize the thermo-viscoelastic properties of polymeric interlayers for laminated glass. Construction and Building Materials 2014;65:1–13.

[20] Williams M, Landel R, Ferry J. The temperature dependence of relaxation mechanisms in amorphous polymers and other glass-forming liquids. Journal of the American Chemical Society 1955;77(14):3701–7.

[21] Gant F, Bower M. Domain of influence method: A new method for approximating prony series coefficients and exponents for viscoelastic materials. Journal of Polymer Engineering 1997;17(1):1–22.

[22] Royer-Carfagni G, Viviani L. Basic design of cable-supported glazed surfaces under blast waves. International Journal of Non-Linear Mechanics 2020;123:art. 103489.

[23] Hooper P, Sukhram R, Blackman B, Dear J. On the blast resistance of laminated glass. International Journal of Solids and Structures 2012;49(6):899 – 918.

[24] Nutting P. A new general law of deformation. Journal of the Franklin Institute 1921;191(5):679–85.

[25] Park S, Kim Y. Fitting Prony-series viscoelastic models with power-law presmoothing. Journal of Materials in Civil Engineering 2001;13(1):26–32.

[26] Gemant A. A method of analyzing experimental results obtained from elastoviscous bodies. Journal of Applied Physics 1936;7(8):311–7.

[27] Bagley R, Torvik P. Fractional calculus. a different approach to the analysis of viscoelastically damped structures. AIAA Journal 1983;21(5):741–8.

[28] Torvik P, Bagley R. On the appearance of the fractional derivative in the behavior of real materials. Journal of Applied Mechanics, Transactions ASME 1984;51(2):294–8.

[29] Bagley R. On the fractional calculus model of viscoelastic behavior. Journal of Rheology 1986;30(1):133–55.

[30] Schiessel H, Blumen A. Hierarchical analogues to fractional relaxation equations. Journal of Physics A: Mathematical and General 1993;26(19):5057–69.

[31] Schiessel H, Metzler R, Blumen A, Nonnenmacher T. Generalized viscoelastic models: Their fractional equations with solutions. Journal of Physics A: General Physics 1995;28(23):6567–84.

[32] Makris N. Three-dimensional constitutive viscoelastic laws with fractional order time derivatives. Journal of Rheology 1997;41(5):1007–20.

[33] Spanos P, Evangelatos G. Response of a non-linear system with restoring forces governed by fractional derivatives-time domain simulation and statistical linearization solution. Soil Dynamics and Earthquake Engineering 2010;30(9):811–21.

[34] Pirrotta A, Cutrona S, Di Lorenzo S. Fractional visco-elastic Timoshenko beam from elastic Euler-Bernoulli beam. Acta Mechanica 2015;226(1):179–89.

[35] Pirrotta A, Cutrona S, Di Lorenzo S, Di Matteo A. Fractional visco-elastic Timoshenko beam deflection via single equation. International Journal for Numerical Methods in Engineering 2015;104(9):869–86.

[36] Di Paola M, Heuer R, Pirrotta A. Fractional visco-elastic Euler-Bernoulli beam. International Journal of Solids and Structures 2013;50(22-23):3505–10.

[37] Di Paola M, Zingales M. Exact mechanical models of fractional hereditary materials. Journal of Rheology 2012;56(5):983–1004.

[38] Alotta G, Barrera O, Cocks A, Paola M. On the behavior of a three-dimensional fractional viscoelastic constitutive model. Meccanica 2017;52(9):2127–42.

[39] Di Paola M, Pirrotta A, Valenza A. Visco-elastic behavior through fractional calculus: An easier method for best fitting experimental results. Mechanics of Materials 2011;43(12):799–806.

[40] Di Paola M, Fiore V, Pinnola F, Valenza A. On the influence of the initial ramp for a correct definition of the parameters of fractional viscoelastic materials. Mechanics of Materials 2014;69(1):63–70.

[41] Atanacković TM, Pilipović S, Stanković B, Zorica D. Fractional calculus with applications in mechanics. London: Wiley; 2014.

[42] Mainardi F. Fractional calculus and waves in linear viscoelasticity: an introduction to mathematical models. London: Imperial College Press; 2010.

[43] Podlubny I. Fractional differential equations. New York: Academic Press; 1999.

[44] Baleanu D, Diethelm K, Scalas E, Trujillo J. In: Fractional Calculus. Models and numerical methods; chap. Chapter 2: A Survey of Numerical Methods for the Solution of Ordinary and Partial Fractional Differential Equations. World Scientific; 2012, p. 39–94.

[45] Colinas-Armijo N, Di Paola M. Step-by-step integration for fractional operators. Communications in Nonlinear Science and Numerical Simulation 2018;59:292–305.

[46] Tarasov V. No violation of the leibniz rule. no fractional derivative. Communications in Nonlinear Science and Numerical Simulation 2013;18(11):2945–8.

[47] Tarasov V. Leibniz rule and fractional derivatives of power functions. Journal of Computational and Nonlinear Dynamics 2016;11(3).

[48] Newmark NM. Test and analysis of composite beams with incomplete interaction. Proc Soc Exp Stress Anal 1951;9(1):75–92.

[49] Biolzi L, Ghittoni C, Fedele R, Rosati G. Experimental and theoretical issues in FRP-concrete bonding. Constr Build Mater 2013;41:182–90.

[50] Alotta G, Di Paola M. Fractional viscoelasticity under combined stress and temperature variations. Lecture Notes in Mechanical Engineering 2020;:1703–17.

[51] Colinas-Armijo N, Di Paola M, Di Matteo A. Fractional viscoelastic behaviour under stochastic temperature process. Probabilistic Engineering Mechanics 2018;54:37–43.